

# Monte Carlo Studies (MCLH Simulations) of the CO–NO Reaction on Disordered Substrates and Their Relation with Experiments

Joaquín Cortés\* and Eliana Valencia

Facultad de Ciencias Físicas y Matemáticas, Universidad de Chile, P.O. Box 2777, Santiago, Chile

Received: June 30, 2003; In Final Form: October 31, 2003

A Monte Carlo study is made of the reduction reaction of NO by CO over a uniform surface and on disordered substrates, some of them fractals, assuming a Langmuir–Hinshelwood mechanism and using experimental kinetics parameters proposed in the literature in the case of Rh as the catalyst. There is good agreement in the pressure and temperature intervals studied between the simulations and the analytic solutions of the mechanism for a uniform substrate. For nonuniform surfaces, in which the kinetics mechanism cannot be solved, MC simulations were used. The production and surface coverage diagrams and their extreme values are analyzed for the different systems, with a scaling seen for maximum CO<sub>2</sub> and N<sub>2</sub> production with the fraction of blocked sites in substrates from percolation clusters. The effect of structural sensitivity, temperature, reaction order, and selectivity for N<sub>2</sub>O, of special interest for experimental work, was also studied.

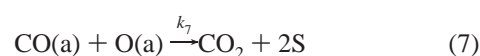
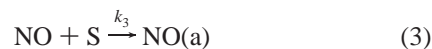
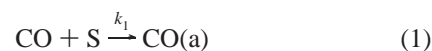
## Introduction

Kinetics models of catalytic reactions are good examples for the study of irreversible dynamics systems that exhibit complicated behaviors, including dissipative structures, oscillations, kinetics phase transitions, etc.<sup>1</sup> This is reflected in the large number of papers in which these kinds of systems have been studied through work that can be roughly classified into two large groups. In the first group, in view of the great complexity of real experimental systems, and with the purpose of using rather accurate mathematical or computer tools, some researchers, usually physicists or mathematicians, would have to be considered to define rather simplified models by analyzing their properties and behaviors. The second group, on the other hand, would address the direct interpretation of the experimental data, and the researchers involved are chemists who study catalysis and face the problem with computer tools and semiempirical theories.

Our group has been interested in these kinds of systems for some years, doing work on both fronts with the purpose of bringing closer together the two approaches whose differences, instead of getting smaller, in our opinion have increased as time goes by. That is the context of this paper, in which we have chosen to study the superficial catalytic reaction of the reduction of NO by CO (CO–NO reaction), which has been used as a type reaction by the two groups mentioned above.

From the experimental viewpoint, the CO–NO reaction, together with the CO oxidation reaction, has been the subject of numerous studies because of its importance in pollution control in catalytic converters. Extensive reviews of the literature on these catalytic systems have been reported by Taylor and by Shelef and Graham,<sup>2</sup> and by Zhdanov and Kasemo.<sup>3</sup> The CO–NO reaction has been shown to be highly complex, and a series of controversies related to their mechanism and to the influence of the structural characteristics of the catalyst's surface have kept alive its present interest in the literature. A series of mechanisms have been proposed since the first papers by Hecker

and Bell,<sup>4</sup> with those of Oh et al.,<sup>5</sup> Cho,<sup>6</sup> and later those of Permana et al.<sup>7</sup> and Peden et al.<sup>8</sup> deserving special mention. The latter, as a result of experimental work on rhodium, proposed the Langmuir–Hinshelwood (LH) mechanism, largely accepted at present, which includes the following steps:



The most important argument until then was centered on the way in which the N<sub>2</sub> and N<sub>2</sub>O products were formed, the latter not having been found initially in the experiments. The other aspect of interest, studied originally by Oh et al.,<sup>9</sup> which we have considered in one of our recent papers,<sup>10</sup> is the structural sensitivity shown by the CO–NO reaction. This aspect, of fundamental interest in the behavior of supported catalysts, recently led C. Chuang and C. Tan<sup>11</sup> to propose a new mechanism that takes into account the experimental existence of the ionic species Rh–NO<sup>+</sup> and Rh–NO<sup>−</sup> on the surface and could describe the behavior of the reaction over supported Rh catalysts. Unfortunately, the studies of this mechanism are too recent and the values of its kinetics constants are not known yet.

\* Corresponding author. E-mail: jcortes@dq.uchile.cl

Theoretically, the monomer–dimer reaction  $A + BC \rightarrow AC + 1/2B_2$ , which mimics the CO–NO reaction, was studied initially by Yaldran and Khan,<sup>12</sup> Brosilow and Ziff,<sup>13</sup> and Meng, Weinberg, and Evans,<sup>14</sup> through Monte Carlo (MC) simulations and mean field theories (MFT) at the sites level, assuming a simplified mechanism which showed an interesting phenomenon of surface poisoning. Later, our group extended the study of this reaction through MFT models at the pairs level for the simplified mechanism<sup>15</sup> and for a complete mechanism,<sup>16</sup> confirming the theoretical results with MC simulations. Recently, Dickmann<sup>17</sup> extended these analyses to different superficial lattices.

The MC simulations and MFT models developed in all these papers assume in general arbitrary specific rate constants for the stages of the assumed kinetics mechanism. The CO–NO reaction has not been studied much through MC simulations that take into account experimental rate constants from activation energies and frequency factors, assuming that the Arrhenius equation is valid, in the way that Araya et al.<sup>18</sup> did for the CO oxidation reaction. In this respect special mention should be made of recent work by Zhdanov and his group,<sup>19</sup> who have considered some particular situations of interest. In general, these studies assume uniform lattices to represent single-crystal catalysts. However, catalysts formed by metal particles constitute disordered systems, perhaps fractals, as has been discussed by some authors<sup>20</sup> and in some of our recent work.<sup>21</sup>

In this paper we shall study the CO–NO reaction, assuming the Peden–Permana mechanism<sup>7,8</sup> for the above equations (1–8) on various disordered theoretical substrates, some of them fractals, by mean of MC simulations and also by means of mean field theory (MFT) at the sites level (LH model) in the case of a uniform surface. The good agreement found between the LH model and MC on uniform surfaces for the pressure and temperature intervals studied in the paper suggests that for disordered surfaces within the same intervals, simulations provide a tool that can be used when an MFT model cannot be applied, which is equivalent to the use of kinetics equations. Henceforth, this procedure will be called the MCLH method. This will make it possible in this paper to study the CO–NO reaction on disordered substrates using kinetics parameters obtained from the experiment, homologating qualitatively real systems such as the example of supported catalysts.

### Simulation Procedure

The MC algorithm used in this paper is similar to one used previously by our group<sup>22</sup> for the CO oxidation reaction, based on one proposed earlier for this system<sup>18</sup> and recently for the CO–NO reaction.<sup>19</sup> For the CO–NO reaction, the simulation process started by selecting an event from the mechanism (1–8) (adsorption, desorption, dissociation, or reaction) according to the probability,  $p_i$ , of the event defined by

$$p_i = k_i / \sum_i k_i \quad (9)$$

where  $k_i$  corresponds to the rate constant of step  $i$  of the mechanism (eqs 1–8). It is assumed that the rate constants  $k_i$  can be expressed as functions of temperature  $T$  according to the Arrhenius equation

$$k_i = \nu_i \exp(-E_i/RT) \quad (10)$$

where  $E_i$  is the activation energy and  $\nu_i$  is the frequency factor.

In the case of adsorption,  $k_i$  was calculated according to the expression of the kinetic theory of gases

$$k_i(\text{ads}) = S_i \sigma (2\pi M_i RT)^{-1/2} \quad (11)$$

where  $M_i$  is the molecular mass of  $i$ ,  $S_i$  is the corresponding sticking coefficient, and the coefficient  $\sigma$  is the area occupied by 1 mole of superficial metal atoms ( $3.75 \times 10^8 \text{ cm}^2/\text{mol}$  for Rh(111)).

The MC algorithm begins with selection of the event. If it corresponds to the adsorption of CO a site is chosen randomly on the surface, and if it is vacant a CO(a) particle will be adsorbed. If the site is occupied, the attempt is ended. If the adsorption of NO is chosen, the procedure is completely analogous and an NO(a) particle is adsorbed.

If CO desorption is chosen, a surface site is selected randomly. If it is occupied by a particle different from CO(a) or it is vacant, the attempt is ended. However, if it is occupied by CO(a) particle, desorption occurs and the particle is replaced by a vacant site. The procedure is analogous in the case of choosing the desorption of NO.

In the case of chemical reaction events, a site on the surface is first chosen randomly. If it is occupied by a particle corresponding to one of the reactions of equations 6–8, a nearest neighbor (nn) site is then chosen randomly next to the first site. If the latter is occupied by the other particle of the same reaction, the event is successful and a product molecule is removed from the surface, leaving two vacant sites. For example, if the first particle is CO(a) and the second is O(a), a molecule of CO<sub>2</sub> leaves the surface.

When the chosen event is the dissociation of NO, a surface site is chosen randomly. If it is occupied by an NO(a) particle, an nn site is chosen randomly next to the first site. If this is empty, dissociation occurs and an N(a) particle remains in the first site and an O(a) particle in the second site. However, if the first site was originally empty and the second nn site is occupied by an NO(a) particle, dissociation occurs and an O(a) particle remains in the first site and an N(a) particle in the second site.

The MC experiments were carried out over a uniform square lattice and over two other kinds of substrates, a deterministic fractal that we have called FRX, and other statistical substrates that we shall call percolation substrates, whose characteristics are described in Appendix 1.

In general, to reach an adequate stability in the results, use was made of a number of iterations of the order of  $10^6$  MCS (Monte Carlo steps), defined as a number of attempts equal to the number of sites in the substrate.

### Reaction Model

The MC studies made in this paper will be analyzed and related to the solution of the classical kinetics equations of the above mechanism (eqs 1–8), called the LH model, which corresponds to an MFT model at the sites level parametrized by the experimental rate constants, a procedure that is usual in the kinetics interpretation of laboratory results. In this respect, we can see that the Peden–Permana mechanism given by equations 1–8 can be solved numerically for the variables corresponding to superficial coverage  $\theta_i$  of species  $i$  (CO, NO,

O, N) which fulfill the following dynamics expressions:

$$\frac{d\theta_{\text{CO}}}{dt} = k_1\theta_{\text{S}}p_{\text{CO}} - k_2\theta_{\text{CO}} - k_7\theta_{\text{CO}}\theta_{\text{O}} \quad (12)$$

$$\frac{d\theta_{\text{NO}}}{dt} = k_3\theta_{\text{S}}p_{\text{NO}} - k_4\theta_{\text{NO}} - k_5\theta_{\text{NO}}\theta_{\text{S}} - k_8\theta_{\text{NO}}\theta_{\text{N}} \quad (13)$$

$$\frac{d\theta_{\text{N}}}{dt} = k_5\theta_{\text{NO}}\theta_{\text{S}} - 2k_6\theta_{\text{N}}^2 - k_8\theta_{\text{NO}}\theta_{\text{N}} \quad (14)$$

$$\frac{d\theta_{\text{O}}}{dt} = k_5\theta_{\text{NO}}\theta_{\text{S}} - k_7\theta_{\text{CO}}\theta_{\text{O}} \quad (15)$$

The time-independent steady-state values of the variables  $\theta_i$  were obtained when integrating numerically from the initial state for  $t \rightarrow 0$  through  $t \rightarrow \infty$ . These results were found to be identical to those of the model's analytic solution, assuming a quasi-equilibrium regime for the adsorption–desorption steps of CO and NO, in the range of the kinetics constants that will be used in this paper. This analytic solution, computationally very useful for making theoretical studies of the model, such as, for instance, analyzing the sensitivity of the parameters or determining their optimum values, will be summarized below for the given case.

If adsorbates CO(a) and NO(a) are in equilibrium with the gas phase, the first four steps (eqs 1–4) can be expressed by the equilibrium relations and

$$\begin{aligned} K_{\text{CO}} &= \frac{\theta_{\text{CO}}}{\theta_{\text{S}}p_{\text{CO}}} \\ K_{\text{NO}} &= \frac{\theta_{\text{NO}}}{\theta_{\text{S}}p_{\text{NO}}} \end{aligned} \quad (16)$$

in which the equilibrium constants  $K_i$  are expressed as functions of the coverages  $\theta_{\text{CO}}$  and  $\theta_{\text{NO}}$  and the partial pressures  $p_{\text{CO}}$  and  $p_{\text{NO}}$  of the gas phase, and where  $\theta_{\text{S}}$  represents the coverage of the unoccupied surface sites, so that

$$\theta_{\text{S}} + \theta_{\text{CO}} + \theta_{\text{NO}} + \theta_{\text{N}} + \theta_{\text{O}} = 1 \quad (17)$$

Considering the steady-state conservation equations from expressions (14) and (15) for the superficial species N(a) and O(a) ( $d\theta_{\text{N}}/dt = 0$ ,  $d\theta_{\text{O}}/dt = 0$ ), it is possible to obtain readily expressions for all the system's coverages  $\theta_i$  as functions of its parameters, the temperature and the partial pressures  $p_{\text{CO}}$  and  $p_{\text{NO}}$  of the reactants:

$$A = \frac{p_{\text{NO}}K_{\text{NO}}}{p_{\text{CO}}K_{\text{CO}}} \quad (18)$$

$$B = \frac{1}{K_{\text{CO}}p_{\text{CO}}} \quad (19)$$

$$C = \left( \frac{-k_8A \pm ((k_8A)^2 + 8k_5k_6AB)^{1/2}}{4k_6} \right) \quad (20)$$

$$D = \frac{k_5AB}{k_7} \quad (21)$$

$$\theta_{\text{CO}} = 1/(1 + A + B + C + D) \quad (22)$$

$$\theta_{\text{NO}} = A\theta_{\text{CO}}, \theta_{\text{S}} = B\theta_{\text{CO}}, \theta_{\text{N}} = C\theta_{\text{CO}}, \theta_{\text{O}} = D\theta_{\text{CO}} \quad (23)$$

TABLE 1: Kinetics Parameters Used in the Paper

event	activation energy $E_i$ (kcal/mol)	frequency factor $\nu_i$ (sec <sup>-1</sup> )	refs
CO desorption	28.536 <sup>a</sup> (31.6)–4.5 $\theta_{\text{CO}}$ –10 $\theta_{\text{N}}$	$1.6 \times 10^{14}$	(5)
NO desorption	29.7	$4.6 \times 10^{14}$	(30)
NO dissociation	17.780 <sup>a</sup> (17.5) + 2 $\theta_{\text{NO}}$	$2.1 \times 10^{10}$	(30)
CO <sub>2</sub> production	14.3	$10^{12}$	(5)
N <sub>2</sub> production	32.6–3 $\theta_{\text{O}}$ –9 $\theta_{\text{N}}$	$4 \times 10^{12}$	(30)
N <sub>2</sub> O production	32.700 <sup>a</sup> (34.1)	$5.3 \times 10^{13}$	(31)

<sup>a</sup> Optimum values obtained with the experimental data of ref 7 (Table 2) for  $T = 623$  K,  $p_{\text{CO}} = p_{\text{NO}} = 8$  Torr,  $\theta_{\text{CO}} = 0.06$ ,  $\theta_{\text{NO}} = 0.5$ .

On the other hand, the productions  $R_i$  are the following:

$$R_{\text{CO}_2} = k_7\theta_{\text{CO}}\theta_{\text{O}} \quad R_{\text{N}_2} = k_6\theta_{\text{N}}^2 \quad R_{\text{N}_2\text{O}} = k_8\theta_{\text{NO}}\theta_{\text{N}} \quad (24)$$

The above development assumes that the rate constants are independent of the fractions  $\theta_i$ . However, as seen in Table 1, which shows the constants  $k_i$  of the mechanism (1–8) obtained from the literature, some constants depend on the coverage  $\theta_i$ . To solve this situation the calculation can be made iteratively, starting from tentative constant initial values of  $k_i$  until the calculated values no longer show changes in the results.

## Results and Discussion

**System Parameters.** With the purpose of studying the behavior of the CO–NO reaction by means of the above MC simulations or the LH model, it is necessary to know the values of the activation energy and the frequency factors of the different steps, assuming that the Arrhenius eq 10 is valid for the rate constants  $k_i$ . This is a classical problem. Since those values are strongly dependent on the experimental conditions, this gives rise to frequent discrepancies in the literature of this subject. The practical difficulty of interpreting kinetics data at moderate and high pressures using  $k_i$  constants usually determined under ultrahigh vacuum (UHV) conditions has been called the pressure gap problem.<sup>23</sup> In an interesting recent paper by Zhdanov and Kasemo,<sup>3</sup> they carried out a study that shows the poor agreement obtained by extrapolating the UHV kinetics to moderate pressures ( $p_{\text{NO}} = p_{\text{CO}} = 0.01$  bar) in the case of the CO–NO reaction on Rh, which is the system of interest in this paper.

There is also another problem. Given a certain mechanism and the equations obtained from solving it either analytically or numerically in terms of a system of differential equations, the production and coverage results of the superficial species have a definite sensitivity to changes in the system's parameters, which in this case are the rate constants dependent on the activation energy and on the frequency factors. In the case of the mechanism of equations 1–8, we have found that some of the optimum parameters  $E_i$  or  $\nu_i$  of the model, obtained numerically by a least squares adjustment to experimental data from the literature or from our laboratory, are strongly sensitive to the small variations in the data caused by the inevitable experimental errors. This makes it difficult to adjust adequately the model to the experimental data if rather large intervals of the gas phase pressure and temperature are considered, explaining why it is usual to find reports of experimental data that are analyzed only qualitatively by the proposed mechanism.

Taking the above into account, we have chosen the set of parameters  $E_i$  and  $\nu_i$ , which appear in Table 1, as a reference for this work. They have a reasonable order of magnitude compared to the experimental data, and we shall assume that there will be no changes in relation to the pressure and temperature ranges considered in our analysis. The choice of a set of parameters sufficiently representative of an experimental

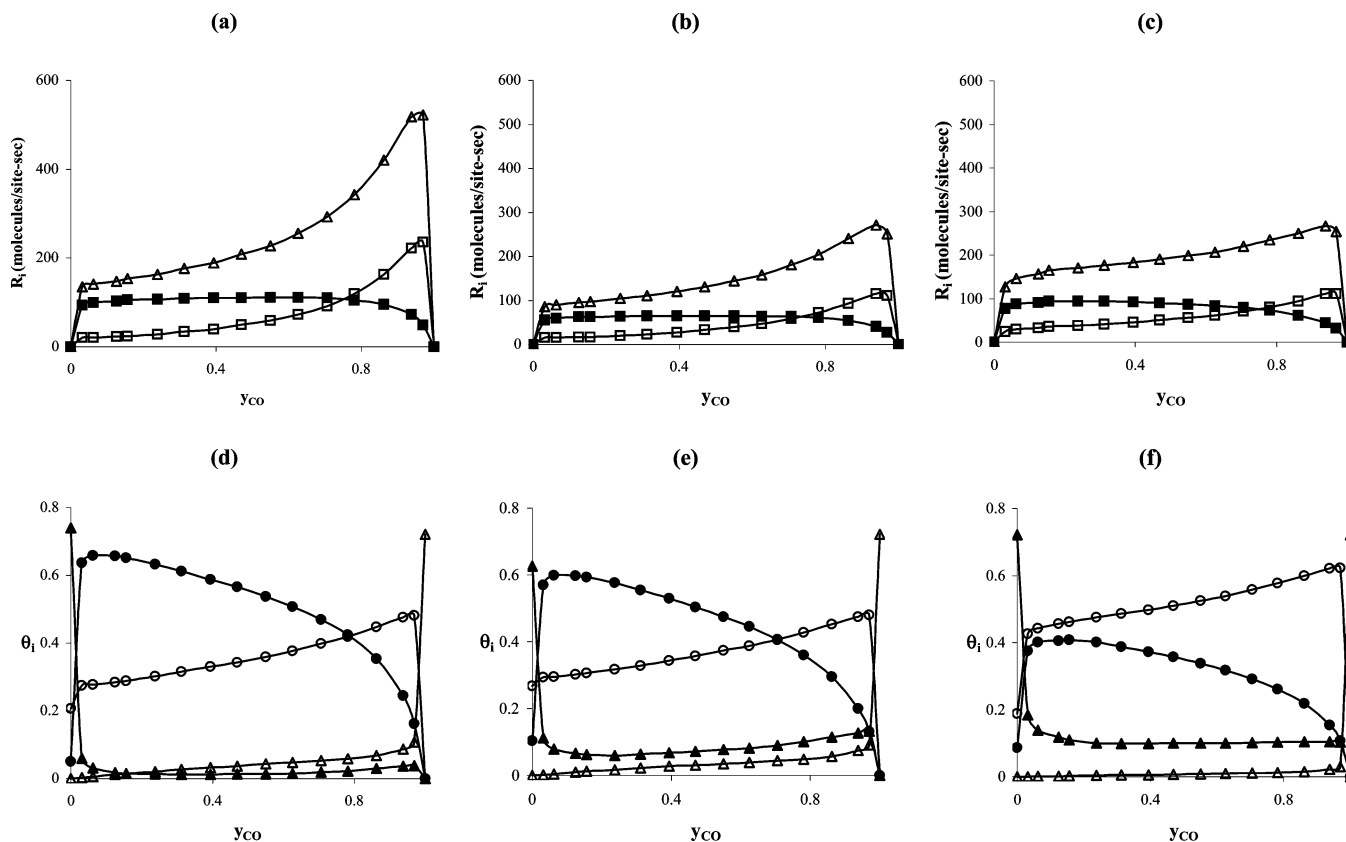


**Figure 1.** Production and coverage diagram obtained by MC for the CO–NO reaction. (a) Production,  $R_i$ , over a uniform surface  $R_{CO_2}$  ( $\Delta$ ),  $R_{N_2O}$  ( $\square$ ),  $R_{N_2}$  ( $\bullet$ ). (b) The same as (a) over an IPC. (c) The same as (a) over FRX. (d) Steady-state concentrations of the different superficial species corresponding to diagram (a)  $\theta_{CO}$  ( $\Delta$ ),  $\theta_O$  ( $\square$ ),  $\theta_N$  ( $\circ$ ),  $\theta_{NO}$  ( $\bullet$ ). (e) The same as (d) corresponding to diagram (b). (f) The same as (d) corresponding to diagram (c). The lines have been drawn to guide the eyes. \* LH results ( $y_{CO} = p_{CO}/(p_{CO} + p_{NO})$ ;  $p_{NO} = 16 - p_{CO}$ ;  $p_{CO} = 10^{-4}$  ( $\theta_o = 0.851$ );  $p_{CO} = 10^{-5}$  ( $\theta_o = 0.977\dots$ );  $p_{CO} = 10^{-8}$  ( $\theta_o = 0.999\dots$ )).

situation will allow us to make a qualitative study of the behavior of theoretical systems that may include various disordered substrates. This makes it possible to carry out analyses that are not too far from actual experiments, something that does not occur frequently in abstract studies of superficial reactions, in an attempt to bring together the two kinds of study groups that were mentioned in the Introduction.

The optimum values for the activation energies of steps 2, 5, and 8 of Table 1 were determined by a least squares adjustment between the kinetics model of the previous section and the experimental data for the values of all the products and the fractions of the surface covered with CO and NO reported by Permana et al.<sup>7</sup> under the same conditions of the table. The remaining parameters shown have been obtained from the literature cited in the table. The procedure has considered as a criterion the doubtful reliability of the parameters of the NO dissociation and  $N_2O$  production steps according to Permana et al.<sup>7</sup> We have also determined the optimum value of the activation energy for the desorption of CO to adjust the coverage values reported in this paper.

In both the above adjustment as well as in the sensitivity analysis of the parameters we have used the analytic solution equations of the previous section, which consider the reasonable assumption of CO and NO equilibria. This assumption has been validated in the pressure and temperature studied intervals, comparing the analytic solutions of our equations with a complete numerical solution that does not include the quasi-equilibrium hypothesis, using the MATLAB software for the calculations. Also, as commented by Zhdanov and Kasemo<sup>3</sup> for instance, the mechanism of the CO–NO reaction over Rh has been discussed in various publications in which several authors

“accept that under steady-state conditions it includes reversible adsorption of NO and CO.”

**Production and Coverage Diagrams.** Figure 1 shows the diagrams determined by MC simulations, given by production  $R_i$  and coverage  $\theta_i$  versus CO concentration in the gas phase,  $y_{CO}$ , at a constant temperature of 650 °C and a total gas-phase pressure  $p_{CO} + p_{NO}$  of 16 Torr, for the CO–NO reaction, assuming that parameters  $E_i$  and  $\nu_i$  of Table 1 are valid. A uniform substrate, the incipient percolation clusters (IPC), and FRX fractals, respectively, were considered, as indicated in a previous section and explained in Appendix 1. The uniform substrate and the IPC have used a reference square lattice of size  $L \times L$ , with  $L = 100$ , and a time of  $10^6$  MCS, averaged over 10 substrates obtained independently in the case of the IPC and the percolation clusters. For the FRX, 4000 elements were considered, and the time needed to reach the steady state was  $2 \times 10^6$  MCS. These values are sufficient for the analysis, since it was confirmed that larger values of  $L$ , the number of substrates, and process time (MCS) do not cause significant changes in the results.

Table 2 shows some results that allow a comparison between the LH model and the MC simulations in the case of a uniform surface. The optimum parameters of Table 1 have been obtained, considering the experimental results of Permana et al.<sup>7</sup> shown in Table 2. The experimental data are also shown in the table in order to visualize the accuracy of both the MC experiment and the LH model in this particular state ( $p_{CO} = p_{NO} = 8$  Torr,  $T = 623$  K), as discussed previously. It is interesting to see in this case the good agreement between the LH model and the MC results because in this temperature and pressure range the relative values of the kinetics parameters in the MC lead to a



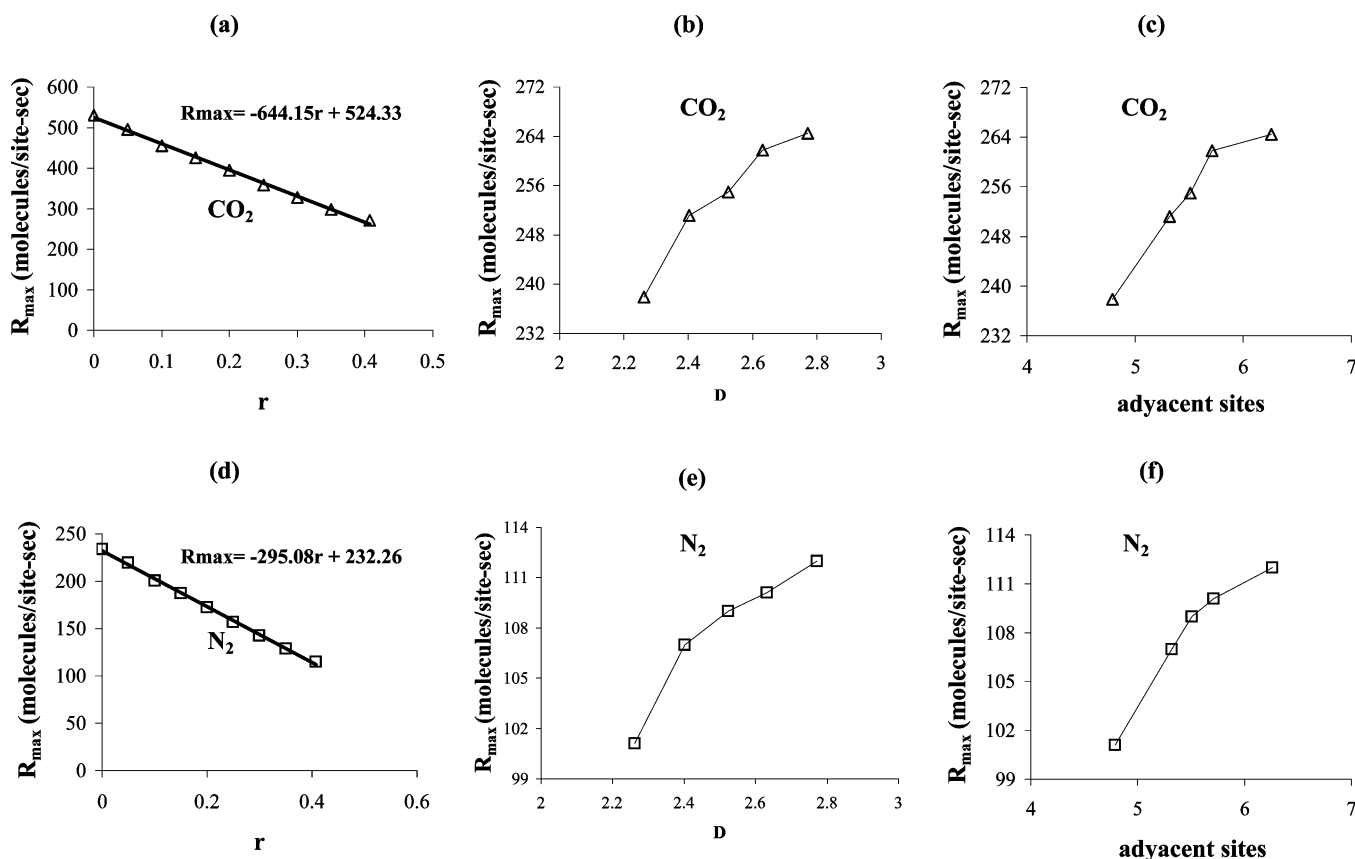


**Figure 2.** (a) Amplitude of  $\text{CO}_2$  production rates,  $R_{\max}$ , as a function of  $r$  fractions of “impurities” of percolation substrates. (b) Amplitude of  $\text{CO}_2$  production rates,  $R_{\max}$ , as a function of fractal dimension  $D$  of FRX substrates. (c) The same as (b) as a function of average number of adjacent sites. (d) The same as (a) but  $R_{\max}$  for  $\text{N}_2$ . (e) The same as (b) but  $R_{\max}$  for  $\text{N}_2$ . (f) The same as (c) but  $R_{\max}$  for  $\text{N}_2$ .

**TABLE 2: Production,  $R_i$  ( $\text{sec}^{-1}$ ), and Coverage  $\theta_i$  for  $T = 623$  K,  $p_{\text{CO}} = p_{\text{NO}} = 8$  Torr, Experimental Data of Ref 7, Monte Carlo (MC), and LH Model**

	exp	assumed optimum parameters from Table 1		assumed constant optimum parameters <sup>a</sup>	
		MC	LH model	MC	LH model
$R_{\text{CO}_2}$	51	47.43	48.53	24.12	24.48
$R_{\text{N}_2}$	8	7.17	8.38	2.41	2.37
$R_{\text{N}_2\text{O}}$	31	33.26	31.76	19.27	19.67
$\theta_{\text{CO}}$	0.06	0.063	0.063	0.310	0.315
$\theta_{\text{NO}}$	0.5	0.637	0.642	0.265	0.271
$\theta_{\text{O}}$	-	$5.48 \times 10^{-3}$	$7.96 \times 10^{-5}$	0.0126	$10^{-5}$
$\theta_{\text{N}}$	-	0.277	0.277	0.405	0.406
$\theta_{\text{E}}$	-	0.0176	0.0176	0.0073	0.0074

<sup>a</sup>  $E_{\text{des CO}} = 28.536$  (kcal/mol),  $E_{\text{dis NO}} = 17.78$  (kcal/mol),  $E_{\text{prod N}_2} = 32.6$  (kcal/mol).

situation of uniformity of the superficial phase, which is what is required by a mean field model, such as the LH, which completely ignores correlations. This is also coherent with the experimental evidence<sup>5</sup> that NO and CO form a well-mixed adlayer, ruling out island formation, as would be, for example, the case of the oxidation reaction of CO. In some of our papers we have also shown how, for this reaction, a mean field theory at the pairs level interprets adequately the MC results.<sup>15,16</sup> Table 2 also shows that the same agreement occurs when the constants  $k_i$  are independent of the coverage. To illustrate this, we have determined the results for the hypothetical case of assuming constant activation energies equal to 28.536 kcal/mol for the desorption of CO, 17.78 kcal/mol for the dispersion of NO, and 32.6 kcal/mol for the production of  $\text{N}_2$ .

The above situation allows the use of the LH model to interpret the (CO–NO) reaction in the case of uniform surfaces

for a given pressure and temperature. This is not possible if the catalytic substrate is disordered, such as in a fractal, because the LH model does not assume the existence of a given substrate. Since this is possible in MC simulations, and the latter agree with the LH model for the uniform system, we have given the name MCLH method to the procedure of studying the qualitative behavior of the CO–NO reaction given the mechanism of equations (1–8) over various disordered substrates by means of the MC simulations described above in the same intervals of pressure and temperature and whose results are shown in the corresponding figures.

If the diagrams of the uniform system are compared with those of the fractal substrate of Figure 1, it is seen that in the latter there is a smaller production of all the products, and this may be associated with the well-known structural sensitivity of this reaction in experiments, in which production decreases with the size of the supported particles. On the other hand, in all the substrates the adsorbed nitrogen coverage remains at intermediate values throughout the diagram, while the adsorbed CO fraction is less than five percent. Both species “expect” the decrease of superficial NO, giving rise to a maximum in the production values. The extremes of the diagram show particular situations which, because of their special interest, will be discussed in greater detail in the next section. The  $\text{CO}_2$  and  $\text{N}_2$  production maxima occur at high gas-phase CO concentrations, while the maximum found in the production of  $\text{N}_2\text{O}$  is not as sharp and occurs at intermediate CO concentrations. Figures 2a and 2d are graphs of the maximum values of  $\text{CO}_2$  and  $\text{N}_2$  production against the fraction  $r$  of surface blocked for the generation of the percolation clusters, as explained in Appendix 1, showing in all cases an interesting and rigorous linearity corresponding to the expression given in the graph.

In the case of the FRX substrate, an increase in maximum CO<sub>2</sub> and N<sub>2</sub> production with the growth of dimension  $D$  of the fractal was seen, as shown in Figures 2b and 2e. Since the greater the fractal dimension the greater its roughness, an improvement in catalytic activity occurs with dimension, due not to the greater surface, since activity is expressed per active site, as explained by Park et al.<sup>24</sup> who studied the ZGB model over the same type of substrate, but to the greater number of next neighbors around the sites located in more corrugated surface regions compared to smoother ones. This promotes the landing probability of NO through step (5) of the mechanism, and offers a better chance for the adsorbed reactant species to encounter a reacting partner. In Figures 2c and 2f we have also graphed production against the average number of adjacent sites.

**Extreme Values of the Coverage Diagram.** Let us discuss first the case corresponding to  $y_{\text{CO}} = 1$ . At that point  $p_{\text{NO}} = 0$ , and the process can then be associated with the first two steps of the mechanism which describes the equilibrium adsorption of CO. The surface consists only of CO particles and empty sites whose values determined by MC were  $x_{\text{CO}} = 0.721$  and  $x_{\text{B}} = 0.279$  for  $p_{\text{CO}} = 16$ . These values are obtained with the LH model in which  $A = C = D = 0$ , so  $\theta_{\text{CO}} = 1/(1+B)$  with  $B = k_2/k_1 p_{\text{CO}}$ , which by the way illustrates from this special case that the coverage diagram is dependent on the total pressure of the gas phase. It is interesting to note that the adsorption of CO requires only one site on the superficial lattice, which explains why at  $y_{\text{CO}} = 1$  the situation is independent of the structure of the substrate, getting the same covered fraction values for the fractals and for the uniform surface.

At the other extreme of the coverage diagram,  $y_{\text{CO}} = 0$  and the NO pressure, which is equal to the total pressure, is  $p_{\text{NO}} = 16$  in this case. Here we have the consequences of NO adsorption on a surface, the steps involved are now (3–6) and (8), and the situation corresponds to the surface with NO, N, and O species and vacant sites. We can see that the values obtained with the MCLH model are different for the uniform substrate and the IPC situations. This is a consequence of the relation between the dissociation and reaction steps and dual nn sites. The neighbor sites of each site, which are four in the case of the uniform surface, are only 2.4 on the average in the case of the branched substrate, which the IPC is. This results in a direct effect on step (5) of NO dissociation and step (6) of N<sub>2</sub> formation.

From the equations of the reaction model section it is clear that if  $p_{\text{NO}} = 0$  the LH model shows a divergence. However, it is possible to attempt the LH calculation for  $y_{\text{CO}}^+$  ( $y_{\text{CO}} \rightarrow 0$ ), some of whose results are given in the figure captions (Figure 1). It is seen that the surface tends to become poisoned with oxygen ( $\theta_{\text{O}} = 1$ ) in contrast with the results of the MCLH, which are certainly the correct ones, since in the calculation of  $y_{\text{CO}}^+$  with the LH model it is necessary to introduce a minimum amount of CO which distorts the calculation.

**Particle Size and the CO–NO Reaction.** As discussed previously, experimental work has shown that the CO–NO reaction experiences structural sensitivity, which becomes evident, for example, in greater production on single-crystal catalysts than on supported ones, and among the latter also greater production on the larger the size of the supported metal particles.<sup>9,10</sup> Among more basic papers, on the other hand, there is simulation work assuming various substrates, including a series of fractals, attempting to mimic supported catalyst situations.<sup>20,21</sup> As already mentioned, Figures 2a and 2d show the results of maximum CO<sub>2</sub> and N<sub>2</sub> production carried out over a series of percolation substrates (Appendix 1) which go from

the extreme of  $r = 0$  (uniform) to  $r = 0.407254$  (IPC). Since substrate branching increases with the value of  $r$ , leading to a decrease in the average number of neighbors around the superficial site,<sup>25</sup> it is possible to associate the increase in  $r$  with the decrease in mean particle size of a supported catalyst. The decreased production of all the products with the value of  $r$  is coherent with the results of the experiment in which production decreases with the mean size of the catalysts' metal particles. Figure 1, for example, shows the lower production in the case of the IPC than in that of the uniform substrate. Selectivity for N<sub>2</sub>O, however, does not change significantly with  $r$ , as shown at two temperatures in Figure 3d, which will be discussed below.

**Effect of Temperature and Pressure on the CO–NO Reaction.** In this section we shall discuss qualitatively some results of our simulations in relation to the trends seen in the experiment. Since the kinetics parameters chosen in the analysis of the paper were adjusted around a state given in Table 1, as mentioned in an earlier section, it is not possible, given the sensitivity of the model, for the LH solutions or the MCLH simulations to interpret quantitatively the experimental data over wide ranges of temperature and pressure. However, as seen in Figure 3, orders of magnitude and trends in agreement with the experiments are obtained.<sup>7,8</sup> This is the case of the increased activity of the system with temperature, with an excellent Arrhenius-type behavior at temperatures below about 700 K in all cases, corresponding to different pressures and substrates, as illustrated in Figure 3a for the production of CO<sub>2</sub> ( $R_{\text{CO}_2}$ ) in the case of the IPC. However, if the apparent activation energy values and the frequency factors are compared with the experimental data of Peden et al.<sup>8</sup> for Rh(111) and Rh(110), the simulated results were greater by at least 30%.

Figures 3b and 3c show the simulated results for the activity of the system against changes in the gas-phase pressure of CO and NO, and Table 3 shows the reaction order for the different cases, calculated assuming a rate law of the  $R_i = k p_{\text{CO}}^m p_{\text{NO}}^n$  type. The values and trends are in agreement with those found experimentally in the literature,<sup>7,8</sup> where zero order is reported for the CO pressure and an order of the kind given in the table for the NO pressure.

Figure 3 also shows the selectivity values for N<sub>2</sub>O,  $S_{\text{N}_2\text{O}}$ , defined by the expression

$$S_{\text{N}_2\text{O}} = \frac{R_{\text{N}_2\text{O}}}{(R_{\text{N}_2\text{O}} + R_{\text{N}_2})} \quad (25)$$

for different  $r$  values, temperatures and pressures studied in some cases. Figure 3d, for example, shows the plot of  $S_{\text{N}_2\text{O}}$  for different values of  $r$  at two temperatures, corresponding to different percolation substrates, which can be associated with experiments with various particle sizes. This agrees with the experiments of Oh et al.<sup>5,9</sup> who find that even though the CO–NO reaction is structurally sensitive, no significant changes in selectivity occur with particle size.

Figure 3e, on the other hand, shows a decrease in selectivity in the temperature range studied, a phenomenon seen experimentally except in some low-temperature cases.<sup>7,8</sup> Figure 3f shows that  $S_{\text{N}_2\text{O}}$  does not undergo any changes in  $p_{\text{CO}}$  if  $p_{\text{NO}}$  remains constant, which is coherent with the results of Figure 3b. Selectivity increases, however, in the region of low  $p_{\text{NO}}$  if  $p_{\text{CO}}$  remains constant, and this differs with what Peden et al.<sup>8</sup> found in some of their experiments.

## Conclusions

By choosing a set of parameters representative of the experiment for the CO–NO reaction, good agreement was found

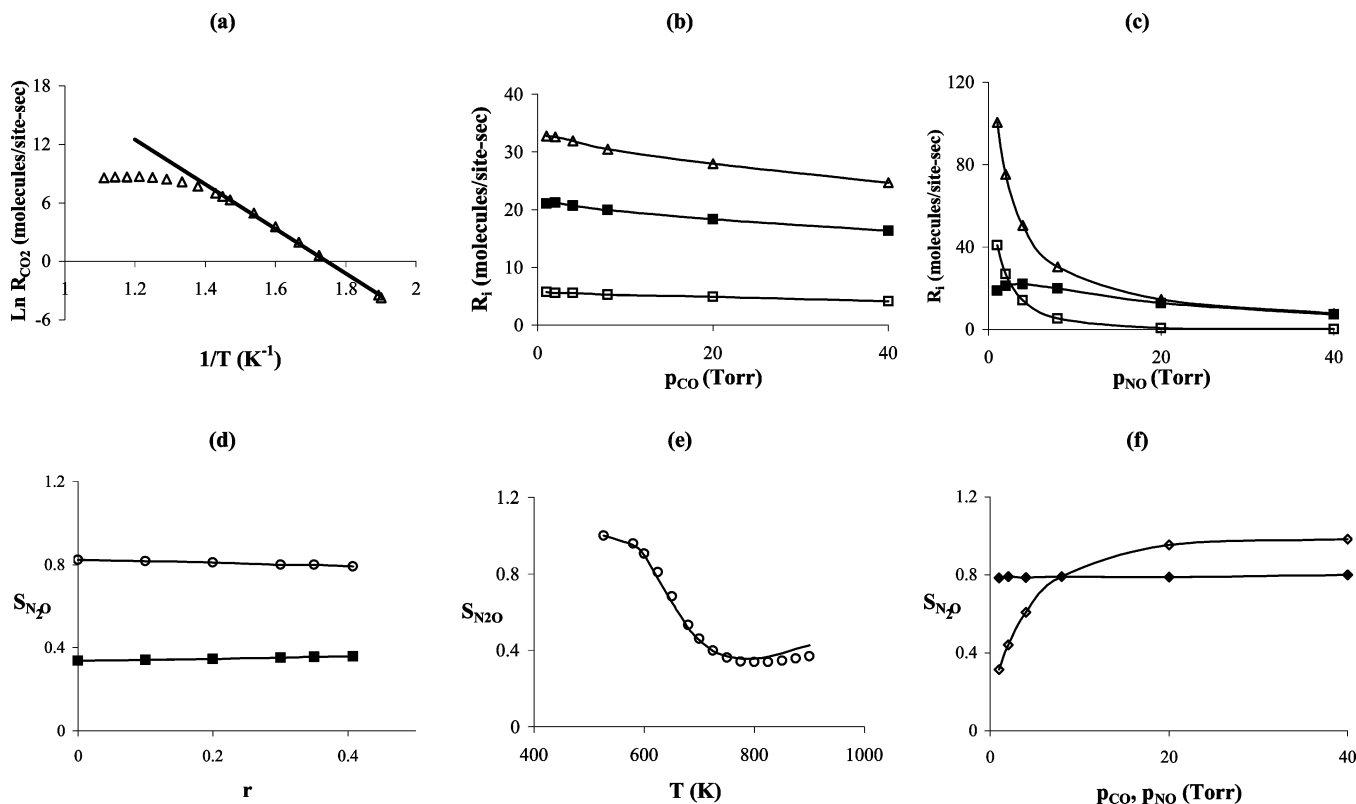


**Figure 3.** (a) Arrhenius-like expression for specific rates of CO<sub>2</sub> formation for the NO–CO reaction over IPC para  $p_{\text{CO}} = p_{\text{NO}} = 8$  Torr. (b) Production,  $R_i$ , as a function of CO pressure with a fixed NO pressure of 8 Torr at 623 K over IPC;  $R_{\text{CO}_2}$  ( $\Delta$ ),  $R_{\text{N}_2}$  ( $\square$ ),  $R_{\text{N}_2\text{O}}$  ( $\blacksquare$ ). (c) Production,  $R_i$ , as a function of NO pressure with a fixed CO pressure of 8 Torr at 623 K over IPC;  $R_{\text{CO}_2}$  ( $\Delta$ ),  $R_{\text{N}_2}$  ( $\square$ ),  $R_{\text{N}_2\text{O}}$  ( $\blacksquare$ ). (d) Selectivity for N<sub>2</sub>O as a function of  $r$  fraction of “impurities” for  $p_{\text{CO}} = p_{\text{NO}} = 8$  Torr,  $T = 623$  K ( $\circ$ ),  $T = 800$  K ( $\blacksquare$ ). (e) Selectivity for N<sub>2</sub>O as a function of temperature  $T$  for  $p_{\text{CO}} = p_{\text{NO}} = 8$  Torr over IPC ( $\circ$ ), uniform surface ( $-$ ). (f) Selectivity for N<sub>2</sub>O as a function of pressure  $p_{\text{CO}}$  ( $\blacklozenge$ ) and  $p_{\text{NO}}$  ( $\blacktriangleright$ ) over IPC for  $T = 623$  K.

**TABLE 3: Reaction Order ( $r = kp_{\text{CO}}^m p_{\text{NO}}^n$ ) at 623 K for the CO–NO System Corresponding to the Data in Figures 3b and 3c**

	$r = 0$ (uniform)	$r = 0.407254$ (IPC)
$m(\text{CO}_2)$	−0.11	−0.13
$m(\text{N}_2)$	−0.07	−0.08
$m(\text{N}_2\text{O})$	−0.12	−0.10
$n(\text{CO}_2)$	−0.81	−0.82
$n(\text{N}_2)$	−2.10	−2.07
$n(\text{N}_2\text{O})$	−0.27	−0.25

between the MC simulations and a mean field model (LH model) in the case of a uniform substrate for the intervals of pressure and temperature studied in the paper. This provides a tool, MCLH simulations, for studying the behavior of the reaction over a variety of disordered theoretical substrates that are representative of, for instance, supported catalysts. Some interesting results were the following.

(i) The structural sensitivity of the CO–NO reaction in experiments (decreased production with decreasing size of the supported particles in real catalysts) can be homologated with the lower production seen in the case of a fractal substrate compared to a uniform one.

(ii) An interesting and rigorous scaling of the CO<sub>2</sub> and N<sub>2</sub> production maxima with the fraction  $r$  of blocked surface of a series of percolation clusters from the uniform surface and the fractal IPC.

(iii) In the case of the FRX substrate the CO<sub>2</sub> and N<sub>2</sub> production maxima increase with the dimension of the fractal, and therefore with surface roughness and the number of neighbor sites adjacent to the active site.

The behavior of the CO–NO reaction on these theoretical disordered substrates reproduces qualitatively a series of trends seen in the experiment, such as the Arrhenius type behavior of production in a certain temperature range, while selectivity toward N<sub>2</sub>O,  $S_{\text{N}_2\text{O}}$ , remains constant with substrate particle size. The values and trends of the reaction order for CO and NO pressure, on the other hand, are in agreement with those found experimentally in the literature.

One of the extreme values of the coverage diagrams allowed the study of the equilibrium adsorption of CO, which is reproduced by the LH model and is independent of the structure of the substrate, since the adsorption of CO requires one site on the superficial lattice. The opposite extreme corresponds to the adsorption of NO, which includes dissociation and reaction on the surface and whose results depend on the structure of the substrate due to the action of the dual nn sites. This case, which corresponds to the  $y_{\text{CO}}^+$  ( $y_{\text{CO}} \rightarrow 0$ ) situation, shows how the results of the MC cannot be reproduced by the MFT due to the divergence seen with the LH model when  $p_{\text{CO}} = 0$ . The MFT shows at the  $p_{\text{CO}} \rightarrow 0$  limit an apparent poisoning of the surface with oxygen ( $\theta_0 = 1$ ) which is, however, the result of an artifact of the mean field model while the MC shows at  $p_{\text{CO}} = 0$  that  $\theta_0 = 0.74$  for the uniform surface.

**Acknowledgment.** The authors thank FONDECYT N°1030759 for financial support of this work.

## Appendix 1

The substrates used in the simulations were a uniform surface made of sites located in an LxL square lattice, a series of substrates that will be called percolation substrates, and a deterministic fractal that will be denoted by FRX.

The active sites corresponding to the percolation substrates are generated by blocking a fraction  $r$  of the  $L \times L$  sites (impurities) of the square lattice, generating catalytic surfaces that go from the extreme of  $r = 0$  (uniform) to  $r = 0.407254$ , which is a statistical fractal called IPC (incipient percolation cluster) with a fractal dimension equal to  $91/48$ .<sup>26</sup> The substrates are obtained by considering only a spanning cluster of the remaining sites computed by Kopelman's algorithm.<sup>27</sup>

Since all the above substrates are probabilistic or nondeterministic, it was necessary to generate a number of them, so that the properties obtained from MC for the CO–NO reaction are the average of the results of the simulations carried out on those substrates.

The FRX substrates were obtained by generating a series of deterministic fractals of different dimensions based on a symmetry theoretical concept of fractal geometry<sup>28</sup> in the same way as the surfaces used by Park et al.<sup>24,29</sup> in MC studies of catalytic CO oxidation. The method consists of the construction of multifractal surfaces by the repetition of self-similar structures within a structure at successively finer length scales, assigning a set of affine transformations  $\{\omega_i\}$  which contract and move the structure, such that the union of these images constitutes the given fractal itself, i.e.,

$$X = \cup_{i=1}^n \omega_i(X) \quad (\text{A1})$$

where  $X$  is the fractal and  $n$  is the number of associated affine transformations.<sup>28</sup> If  $\lambda_i$  is the scaling factor of the  $i$ th affine transformation,  $\omega_i$ , it is possible to determine the dimension  $D$  of the fractal from the relation

$$\sum_{i=1}^n \lambda_i^D = 1 \quad (\text{A2})$$

In our work we consider a fractal support defined by sets of affine transformations of the form

$$\omega_i \begin{pmatrix} x \\ y \\ z \end{pmatrix} = \lambda_i \begin{pmatrix} \cos\theta_i & -\sin\theta_i & 0 \\ \sin\theta_i & \cos\theta_i & 0 \\ 0 & 0 & 1 \end{pmatrix} \begin{pmatrix} x \\ y \\ z \end{pmatrix} + \begin{pmatrix} l_i \\ m_i \\ n_i \end{pmatrix} \quad (\text{A3})$$

considering the scaling factor  $\lambda_i$  equal to  $1/3$  in all of them. The values of the rotational angles  $\theta_i$  and the translations  $l_i$ ,  $m_i$  and  $n_i$  in the respective  $x$ ,  $y$ , and  $z$  directions were those given in Table 1 of ref 24. In general, fractals of different dimension can be obtained by changing the number of affine transformations and the associated scaling factors.

To construct the fractals on the computer, use was made of the random iteration algorithm<sup>24,29</sup> as follows: a sequence of spatial points  $\{\mathbf{r}_N: N = 0, 1, 2, \dots\}$  is generated recursively by applying the transformation

$$\mathbf{r}_N = \omega_i(\mathbf{r}_{N-1}) \quad (\text{A4})$$

from any point  $\mathbf{r}_0$  in space, e.g., the origin. At each step, a particular transformation, say  $\omega_i$ , is selected with an assigned

probability  $p_i$  from an arbitrary set  $\{p_i\}$  such that  $\sum_i p_i = 1$ . In our case 4000 points were generated in this way, becoming the active sites of the FRX substrates. Neighbors of a site of the FRX fractal are considered to be all those fractal sites located in a spherical environment of radius  $R$  determined, following Park et al.,<sup>24,29</sup> as twice the average distance between every surface site and its nearest neighbor.

## References and Notes

- (1) Nicolis, G.; Prigogine, I., *Self-Organization in Nonequilibrium Systems*, Wiley-Interscience: New York, 1977. Haken, H., *Synergetics*; Springer-Verlag: New York, 1977. Marro, J.; Dickman, R., *Nonequilibrium Phase Transitions in Lattice Models*; University Press: Cambridge, 1999.
- (2) Taylor, K. C. *Catal. Rev. Sci. Eng.* **1993**, *35*, 457. Shelef, M.; Graham, G. *Catal. Rev. Sci. Eng.* **1994**, *36*, 433.
- (3) Zhdanov, V. P.; Kasemo, B. *Surf. Sci. Rep.* **1997**, *29*, 31.
- (4) Hecker, W. C.; Bell, A. T. *J. Catal.* **1983**, *84*, 200.
- (5) Oh, S. H.; Fisher, G. B.; Carpenter, J. E.; Wayne, D. J. *Catal.* **1986**, *100*, 360.
- (6) Cho, B. K. *J. Catal.* **1992**, *138*, 255. Cho, B. K. *J. Catal.* **1994**, *148*, 697.
- (7) Permana, H.; Simon Ng, K.; Peden, Ch.; Schmieg, S. J.; Lambert, D. K.; Belton, D. J. *Catal.* **1996**, *164*, 194.
- (8) Peden, Ch.; Belton, D.; Schmieg, S. J. *J. Catal.* **1995**, *155*, 204.
- (9) Oh, S. H.; Eickel, C. C. *J. Catal.* **1991**, *128*, 526.
- (10) Araya, P.; Gracia, F.; Cortés, J.; Wolf, E. *Appl. Catal. B* **2002**, *997*, 1–4.
- (11) Chuang, S.; Tan, C. J. *Catal.* **1998**, *173*, 95.
- (12) Yaldram, K.; Khan, M. A. J. *Catal.* **1991**, *131*, 369.
- (13) Brosilow, B. J.; Ziff, R. M. *J. Catal.* **1992**, *136*, 275.
- (14) Meng, B.; Wienberg, W. H.; Evans, J. W. *Phys. Rev. E* **1993**, *48*, 3577.
- (15) Cortés, J.; Puschmann, H.; Valencia, E. J. *Chem. Phys.* **1996**, *105*, 6026.
- (16) Cortés, J.; Puschmann, H.; Valencia, E. J. *Chem. Phys.* **1998**, *109*, 6086.
- (17) Dickman, A. G.; Grandi, B. C. S.; Figueiredo, W.; Dickman, R. *Phys. Rev.* **1999**, *E59*, 6361.
- (18) Araya, P.; Porod, W.; Wolf, E. *Surf. Sci.* **1990**, *230*, 245. Araya, P.; Porod, W.; Sant, R.; Wolf, E. *Surf. Sci.* **1989**, *L80*, 208.
- (19) Olsson, L.; Zhdanov, V. P.; Kasemo, B. *Surf. Sci.* **2003**, *529*, 338.
- (20) Albano, E. V. *Hetero. Chem. Rev.* **1996**, *3*, 389. Albano, E. V. In *Computational Methods in Surface and Colloid Science*; M. Borówko, Ed.; Marcel Dekker: New York, 2000; Chapter 8. Hovi, J. P.; Vaari, J.; Kaukonen, H. P.; Nieminen, R. E. *Comput. Mater. Sci.* **1992**, *1*, 33; Loscar, E.; Albano, E. V. *Rep. Prog. Phys.* **2003**, *66*, 1343.
- (21) Valencia, E.; Cortés, J.; Puschmann, H. *Surf. Sci.* **2000**, *470*, L109. Cortés, J.; Valencia, E. *Physica A* **2002**, *309*, 628. Cortés, J.; Valencia, E. *J. Colloid Interface Sci.* **2002**, *252*, 256. Cortés, J.; Valencia, E. *Can. J. Phys.* **2003**, *81*, 1. Cortés, J.; Jimenez, R.; Araya, P. *Catal. Lett.* **2002**, *82*, 255. Cortés, J.; Narváez, A.; Puschmann, H.; Valencia, E. *Chem. Phys.* **2003**, *288*, 77.
- (22) Cortés, J.; Valencia, E.; Araya, P. *J. Chem. Phys.* **1998**, *109*, 5607.
- (23) Prevot, G.; Meerson, O.; Piccolo, L.; Henry, C. R. *J. Phys.: Condens. Matter* **2002**, *14*, 4251.
- (24) Park, H.; Kim, H.; Lee, S. *Surf. Sci.* **1997**, *380*, 514.
- (25) Casties, A.; Mai, J.; von Niessen, W. *J. Chem. Phys.* **1993**, *99*, 3082.
- (26) Stauffer, D.; Aharony, A. *Introduction to Percolation Theory*, 2nd ed.; Taylor and Francis: London, 1992.
- (27) Hoshen, J.; Kopelman, R. *Phys. Rev. B* **1976**, *14*, 3438. Kopelman, R. *J. Stat. Phys.* **1986**, *42*, 185.
- (28) Barnsley, M. F. *Fractals Everywhere*; Academic Press: New York, 1988. Barnsley M. In *Proceedings of Symposia in Applied Mathematics*; AMS, 1988; Vol 39.
- (29) Park, H.; Lee, S. *Surf. Sci.* **1998**, *411*, 1.
- (30) Belton, D.; DiMaggio, C. L.; Schmieg, S. J.; Simon Ng, K. J. *Catal.* **1997**, *157*, 559.
- (31) Walker, A. V.; Gruyters, M.; King, D. A. *Surf. Sci.* **1997**, *384*, L791.